Bioorganic & Medicinal Chemistry 18 (2010) 3187–3197

Contents lists available at ScienceDirect

Bioorganic & Medicinal Chemistry

journal homepage: www.elsevier.com/locate/bmc

Design, synthesis, biological evaluation and computational investigation of novel inhibitors of dihydrofolate reductase of opportunistic pathogens

Seema Bag [a], Nilesh R. Tawari [a], Mariam S. Degani [a,*], Sherry F. Queener [b]

[a] Department of Pharmaceutical Sciences and Technology, Institute of Chemical Technology, Matunga (E), Mumbai 400 019, India
[b] Department of Pharmacology and Toxicology, Indiana University School of Medicine, Indianapolis, IN 46202, USA

ARTICLE INFO

Article history:
Received 12 January 2010
Revised 12 March 2010
Accepted 13 March 2010
Available online 18 March 2010

Keywords:
Dihydrofolate reductase
2,4-Diaminopyrimidine
Docking
MM-GBSA

ABSTRACT

The present work deals with design, synthesis and biological evaluation of novel, diverse compounds as potential inhibitors of dihydrofolate reductase (DHFR) from opportunistic microorganisms; *Pneumocystis carinii* (pc), *Toxoplasma gondii* (tg) and *Mycobacterium avium* (ma). A set of 14 structurally diverse compounds were designed with varying key pharmacophoric features of DHFR inhibitors, bulky distal substitutions and different bridges joining the distal part and 2,4-diaminopyrimidine nucleus. The designed compounds were synthesized and evaluated in enzyme assay against pc, tg and ma DHFR. The rat liver (rl) DHFR was used as mammalian standard. As the next logical step of the project, flexible molecular docking studies were carried out to predict the binding modes of these compounds in pcDHFR active site and the obtained docked poses were post processed using MM-GBSA protocol for prediction of relative binding affinity. The predicted binding modes were able to rationalize the experimental results in most cases. Of particular interest, both the docking scores and MM-GBSA predicted ΔG_{bind} were able to distinguish between the active and low active compounds. Furthermore, good correlation coefficient of 0.797 was obtained between the IC_{50} values and MM-GBSA predicted ΔG_{bind}. Taken together, the current work provides not only a novel scaffold for further optimization of DHFR inhibitors but also an understanding of the specific interactions of inhibitors with DHFR and structural modifications that improve selectivity.

1. Introduction

Immunocompromised hosts such as HIV positive people are often prone to life threatening infections caused by opportunistic microorganisms including *Pneumocystis carinii* (pc), *Toxoplasma gondii* (tg), and *Mycobacterium avium* (ma).[1] Dihydrofolate reductase (DHFR), a NADPH dependent enzyme, catalyses the crucial reaction of conversion of folic acid to dihydro and tetrahydro folic acid (a cofactor involved in one carbon donation in purine and pyrimidine de novo synthesis) both in mammals as well as microorganisms. Inhibitors of DHFR, which is essential for cell growth and division, have been in clinical use for over 50 years for anticancer (methotrexate), antibacterial (trimethoprim) and antiprotozoal (pyrimethamine) treatments. Current therapeutic treatment for infections caused by pc and tg include co-administration of the selective but weak DHFR inhibitor, trimethoprim or pyrimethamine, in combination with sulfonamides to enhance potency.[2] However, side effects related to sulfonamides is often a serious problem in this treatment. In addition, non-classical antifolates, trimetrexate and piritrexim co-administered with leucovorin for host rescue are also used for the treatment of these infections.[2] However, often, toxicity forces the termination of treatment. DHFR inhibitors are yet to be clinically applied for the treatment of infections caused by ma. Thus, DHFR inhibitors with high potency and selectivity are desired for the treatment of infections caused by these pathogenic organisms.

The presence of overall structurally conserved DHFR in both humans and microorganisms makes the drug design process for antifolates challenging. Several laboratories continue to work towards the search for potent and selective DHFR inhibitors against opportunistic microorganisms. Rosowsky et al. have reported structure based drug design of several novel inhibitors with a bulky tricyclic moiety at 6-position of the 2,4-diaminopteridine nucleus.[3] In a subsequent study, the 3D structure of the ternary complex of one of these inhibitors, 6-((5*H*-dibenzo[*b*,*f*]azepin-5-yl)methyl)pteridine-2,4-diamine, **I**, (Fig. 1) and NADPH with pcDHFR was analyzed using crystallography, highlighting an unusual role of the dibenz[*b*,*f*]-azepine moiety in positioning the diaminopteridine within the active site (PDB code: IKLK).[4] Attempts were made to further enhance potency of this inhibitor, **I**, by replacing the pteridine ring with a pyrido[2,3-*d*]pyrimidine or quinazoline ring, or

Abbreviations: pc, *Pneumocystis carinii*; tg, *Toxoplasma gondii*; DHFR, dihydrofolate reductase; HIV, human immunodeficiency virus; ma, *Mycobacterium avium*.

* Corresponding author. Tel.: +91 22 33612213; fax: +91 22 24145614.
E-mail address: ms.degani@ictmumbai.edu.in (M.S. Degani).

0968-0896/$ - see front matter © 2010 Elsevier Ltd. All rights reserved.
doi:10.1016/j.bmc.2010.03.031

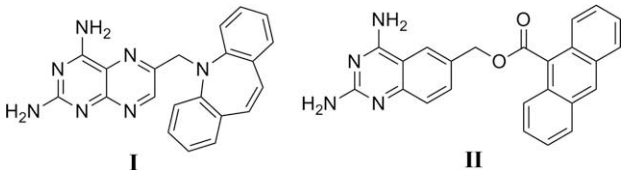

Figure 1. Structures of some of the lipophilic DHFR inhibitors reported in literature.

by changing the azepine ring nitrogen and –CH=CH– bridge by different isosteres. However, these studies did not yield encouraging results.[5] Furthermore, 2′-position of the dibenz[*b*,*f*]azepine ring was substituted with carboxylic acid side chain to improve potency and selectivity.[6] Another approach by Graffner-Nordberg et al. included design, synthesis and computational affinity prediction of ester soft drugs with lipophilic tricyclic ring, **II**, (Fig. 1) substituted on 2,4-diaminoquinazoline nucleus as DHFR inhibitors.[7]

Our research group has been recently involved in the search for novel DHFR inhibitors. Towards this goal we have reported molecular modeling studies against maDHFR to get an insight into the potential features required for maDHFR inhibition.[8] Initially, we have reported a series of extended biguanides and dihydrotriazines as potential DHFR inhibitors against opportunistic microorganisms.[9] Furthermore, based on virtual screening experiments, we have designed and evaluated novel 2-hydrazino-pyrimidin-4(3*H*)-one derivatives, lacking conventional 2,4-diaminopyrimidine nucleus as inhibitors of DHFR from opportunistic microorganisms.[10] While several synthesized compounds showed promising in vitro activity against microbial DHFR, many of these compounds were also equipotent inhibitors of mammalian DHFR thereby decreasing their usefulness.

The current study was aimed at synthesis and biological evaluation of a diverse set of molecules followed by their molecular modeling studies for the understanding of specific interactions of the inhibitors with DHFR and structural modifications that improve selectivity. In this light, based on the literature reports[3–6] and understanding of DHFR active site, a set of 14 structurally diverse compounds was designed; with varying the nitrogen containing heterocycle, bulky tricyclic distal substitutions or different bridges joining the distal part and 2,4-diaminopyrimidine nucleus. Thus, compounds, **3a–c**, were specifically designed in order to check the effect of addition of bulky tricyclic moiety on our newly proposed pharmacophore; 2,4-diamino *s*-triazine for inhibitors of DHFR from opportunistic microorganisms, which structurally mimics the conventional 2,4-diaminopyrimidine pharmacophore of DHFR. The 2,4-diamino groups on *s*-triazine are expected to form crucial H-bonding interactions with conserved residues at active site of DHFR. Using pharmacophoric features of trimethoprim, compounds **8a–b**, were designed with the bulky dibenz[*b*,*f*]azepine and dihydrodibenz[*b*,*f*]azepine moiety substituted on 2,4-diaminopyrimidine moiety. In an attempt to probe steric and electronic tolerance of the DHFR binding pocket, compounds, **5a–b**, **7a** and **8c–d**, were designed with various bridges joining the distal hydrophobic substitution and 2,4-diaminopyrimidine ring system. Compounds, **6a–b**, were designed with conformationally constrained bridge which could possibly lock the 2,4-diaminopyrimidine nucleus and distal substitution in preferred binding orientation. Compounds, **11a–b**, were designed with 6-substituted 2,4-diaminopyrimidine nucleus.

2. Results and discussion

2.1. Synthesis

s-Triazine analogs **3a–c**, were synthesized using the route shown in Scheme 1. This involved N-alkylation of the tricyclic nucleus (**1a–c**). The dihydroiminostilbene (**1a**) was reacted with chloroacetonitrile using K_2CO_3 as a base and heating the reaction mixture in presence of catalytic amount of PEG 6000 and water.[11] The column purified product was then reacted with dicyandiamide in presence of KOH, water using 2-methoxyethanol as solvent to afford target compound **3a**. N-Alkylation of 10*H*-phenothiazine (**1b**) and 2-chloro-10*H*-phenothiazine (**1c**) were carried out using NaH as base and DMSO/DMF as solvent.[12] After column purification, these were reacted with dicyandiamide, using 2-methoxyethanol as solvent to synthesize the desired *s*-triazines (**3b**, **3c**).[13]

The starting material 2,4-diamino-5-cyano pyrimidine (**5**, Scheme 2) was synthesized by reacting guanidine and ethoxymethylene malononitrile according to the method reported by Huber.[14] Molecules **5a** and **5b** were synthesized from 2,4-diamino-5-cyano pyrimidine (**5**, Scheme 2) using reductive alkylation in presence of Raney nickel.[15] 2,4-Diamino-5-cyano pyrimidine (**5**, Scheme 2) was converted to 2,4-diaminopyrimidine-5-carboxaldehyde (**6**, Scheme 2) using Raney nickel with 98–100% formic acid as a solvent.[14–17]

Compounds **6a** and **6b** were synthesized from 2,4-diaminopyrimidine-5-carboxaldehyde (**6**, Scheme 2) by Claisen–Schmidt condensation. 2,4-Diamino-5-carboxaldhyde (**6**, Scheme 2) was reduced to (2,4-diamonopyrimidine-5-yl) methanol (**7**, Scheme 2) using $NaBH_4$. $NaBH_4$ (1.5 equiv) in 100 ml methanol were required for reduction as **6** was sparingly soluble in solvent. It was observed that more than 1 equiv of $NaBH_4$ was required for the completion of the reaction. Compound **7a** was synthesized from (2,4-diamonopyrimidine-5-yl) methanol (**7**, Scheme 2) and naphthalene-2-sulfonyl chloride employing triethylamine as catalyst. 5-(Bromomethyl)pyrimidine-2,4-diamine (**8**, Scheme 2) was synthesized from (2,4-diamonopyrimidine-5-yl) methanol (**7**, Scheme 2) using HBr in glacial acetic acid.[18] The product formed **8**, was highly unstable, therefore immediate azeotropic distillation to remove solvent was followed by next reaction without characterization.

Synthesis of **8a–b** involved N-alkylation of tricyclic ring system. The reaction was performed under inert atmosphere with NaH in dry solvents. Compounds, **8c–d**, were synthesized by using reaction of 5-(bromomethyl)pyrimidine-2,4-diamine (**8**, Scheme 2)

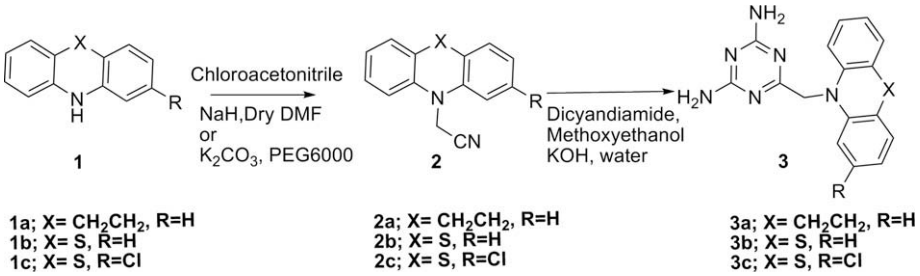

Scheme 1. Scheme for the synthesis of lipophilic *s*-triazine analogs.

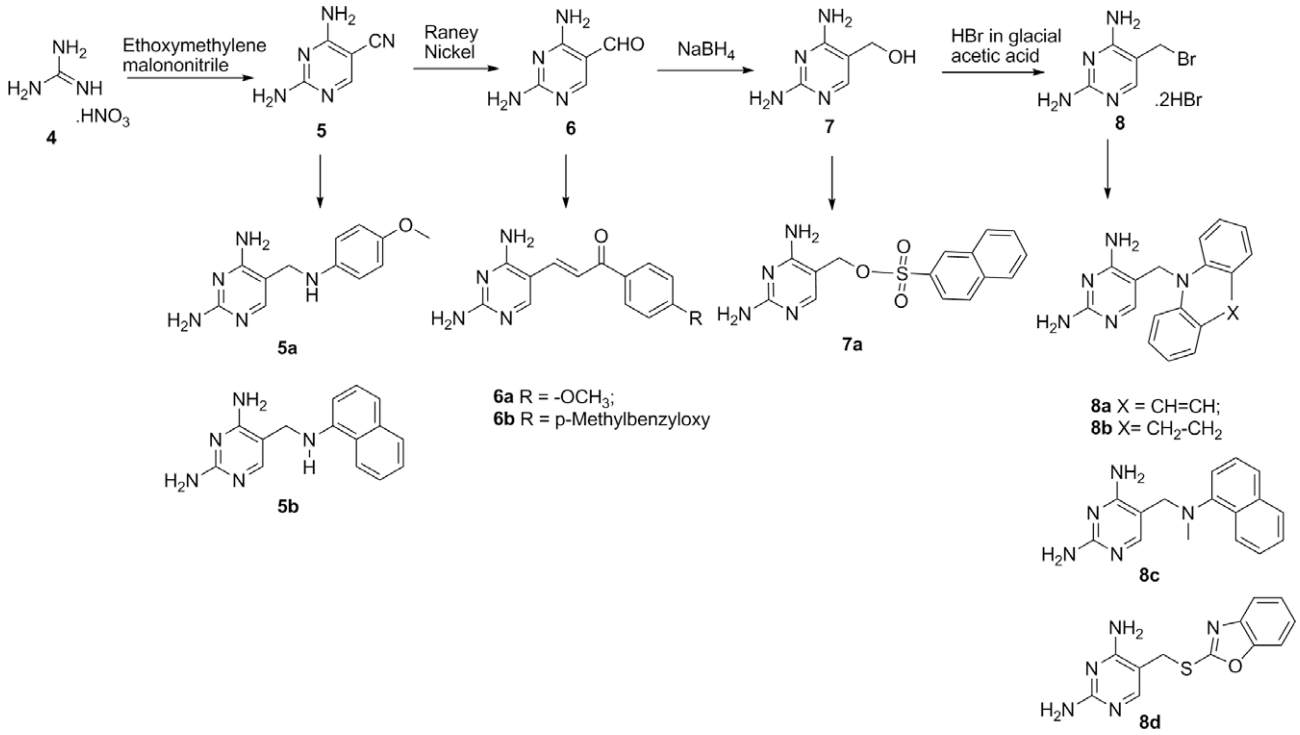

Scheme 2. Scheme for the synthesis of 2,4-pyrimidine analogs.

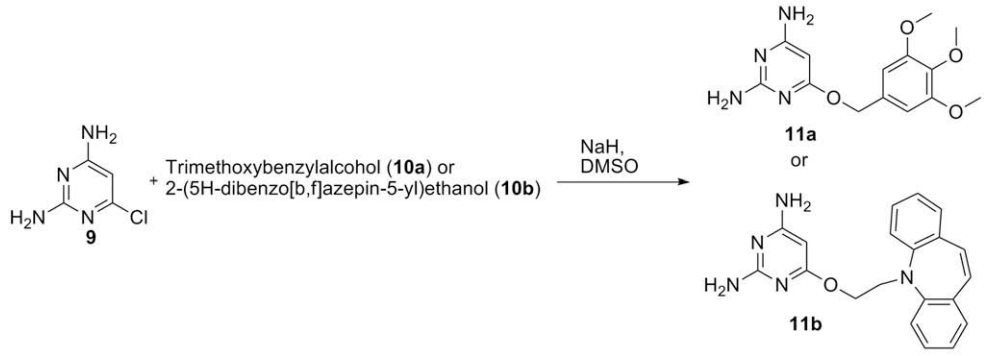

Scheme 3.

with *N*-methylnaphthalen-1-amine[19] and mercaptobenzoxazole. Reaction of 4-chloro-2,6-diaminopyrimidine with the appropriate sodium alkoxide (ROH, NaH, DMSO, 100 °C) afforded corresponding O^4-substituted pyrimidines, **11a–b**, (Scheme 3).

2.2. Biology

The synthesized compounds were evaluated for their ability to inhibit DHFR of pc, tg, ma and rat liver (rl).[20,21] The rl DHFR was used as mammalian standard as it shares high sequence similarity to human DHFR. The data for the reported compounds (trimethprim, I and II) are taken from literature reports[3,7] for comparative purpose. IC_{50} values for all analogs are given in Table 1.

Biological activity results revealed that the synthesized *s*-triazine analogs, **3a–c**, were less active against all DHFRs. These compounds were able to inhibit pcDHFR at concentrations from ~600 to 1200 μM. Only one compound, **3c**, was able to inhibit tgDHFR at ~400 μM concentration. In contrast, the molecules, **8a–b**, with bulky tricyclic substitutions on 2,4-diaminopyrimidine ring system were good inhibitors of microbial DHFRs. Furthermore, these compounds were also found to be selective inhibitors of microbial DHFR compared to rat liver DHFR. In particular, compound, **8b**, inhibited all microbial DHFRs with some selectivity at concentration <1 μM.

Compounds, **5a–b**, and **8c** were designed by incorporating an electronegative nitrogen atom as part of bridge joining the 2,4-diaminopyrimidine ring system and distal substitution. Compound, **5a**, was able to inhibit pcDHFR at concentration of ~363 μM. However, compound, **5b**, with a bulky napthyl substitution at distal part was found to be a better pcDHFR inhibitor with IC_{50} of ~150 μM. Compound, **5b**, also showed inhibition of tgDHFR at ~20 μM with over ~6-fold selectivity to that of rat liver DHFR. Interestingly, addition of a methyl group on the bridge nitrogen atom caused dramatic increase in DHFR inhibitory activity as evident from compound, **8c**, which showed inhibition of maDHFR at concentration < 1 μM with > 200-fold selectivity over rat liver DHFR.

Compounds, **6a–b**, were not found to be inhibitors of DHFR, one of the possible reasons for this behavior could be high conformational restriction owing to presence of α,β-unsaturated carbonyl bridge.

Table 1
Inhibitory concentration (IC_{50} μM) against rlDHFR, pcDHFR, tgDHFR and maDHFR and selectivity ratios versus rlDHFR by target compounds

Mol ID	MW	Activity (μM)				Selectivity		
		pc	tg	ma	rl	rl/pc	rl/tg	rl/ma
3a	318.4	1265.15	139.770 (10)	138.199 (9)	139.77 (0)	ND	ND	ND
3b	322.4	235.46	142.684 (15)	142.684 (4)	142.68 (16)	ND	ND	ND
3c	356.8	603.65	397.11	117.703 (5)	117.7 (8)	ND	ND	ND
5a	245.3	363.26	44.031 (7)	44.031 (0)	44.03 (0)	ND	ND	ND
5b	265.3	150.58	22.13	79.152 (9)	127.85	0.85	5.78	ND
6a	270.3	151.319 (4)	151.318 (15)	151.318 (14)	127.42	ND	ND	ND
6b	360.4	11.653 (2)	116.533 (10)	11.653 (4)	178.130 (0)	ND	ND	ND
7a	330.4	7.88	124.107 (13)	124.107 (15)	124.107 (0)	>15.73	ND	ND
8a	315.4	26.25	8.07	6.35	130.00 (15)	>5	>16	>20
8b	317.4	0.84	0.14	0.11	1.60	1.89	11.48	14.36
8c	279.3	38.48	3.49	0.88	184.26	4.79	52.74	209.312
8d	273.3	35.83	160.22	23.14	520.65	14.53	3.25	22.50
11a	306.1	148.635 (0)	145.272 (10)	145.370 (12)	148.635 (12)	ND	ND	ND
11b	345.4	112.02	3.35	2.33	119.861 (39)	ND	>35.77	>51.44
TMP[a]	—	13	2.80	0.30	180	14	65	600
I[a]	—	0.21	0.043	0.012	4.4	21	102	367
II[a]	—	0.49	0.67	1.0	0.21	0.43	0.31	0.21

Triplicate assays were performed as previously described.[20,21]
Number in parentheses indicates percent inhibition obtained at that concentration.
[a] Data taken from Refs. 3,7.

Compounds, **7a** and **8d**, with electronegative bridges between 2,4-diaminopyrimidine ring system and distal substitution showed modest DHFR inhibitory activity. Of particular interest, compound, 7**a**, was found to be selective for pcDHFR with approximately two-fold increase in activity and good selectivity when compared to trimethoprim.

Among the compounds, **11a–b**, compound **11a** was found to be inactive in all species. However, compound, **11b**, has shown interesting activity of <5 μM against tg and ma DHFR with good selectivity.

2.3. Computational studies

To understand the forms of interactions of synthesized compounds with enzyme and to identify the binding modes of these compounds, we created an accurate docking model for pcDHFR. pcDHFR was selected as the enzyme of choice as the experimentally determined crystal structure of the enzyme was available in public domain. One of the most important considerations in docking simulations is selection of appropriate docking algorithm and scoring function. To evaluate the effectiveness of Glide protocol in flexible docking of DHFR inhibitors, the model of pcDHFR derived from crystallographic data (PDB ID: 1KLK) extending to 2.3 Å resolution for a ternary complex containing a bound molecule of NADPH and an DHFR inhibitor **I**, was selected as the docking receptor. The model preparation and docking studies were carried out using the protocol outlined in the experimental section. Since, DHFR has a highly conserved ligand binding orientation (Fig. 2), 'must match' of at least one hydrogen bond criteria; with Ile123, Ile10 and Glu32 residues was constrained during docking simulations. Using flexible docking procedure in Glide-XP, the observed crystallographic structure was reproduced with RMSD value of 0.65 Å indicating that this docking method is valid and can be used for predicting binding modes of pcDHFR inhibitors. Once the docking algorithm was validated, studies were further extended for molecular docking of synthesized molecules in the active site of pcDHFR. The top scoring poses returned by XP scoring function were analyzed using Maestro graphical interface.

In compounds, **3a–c** and **8a–b**, bulky tricyclic moiety showed desirable hydrophobic interactions with the hydrophobic residues Leu32, Ile65, Phe69, Leu25 and Ile33 in the distal part of active site. However, compound, **3a**, (Fig. 3**a**) did not show any interaction

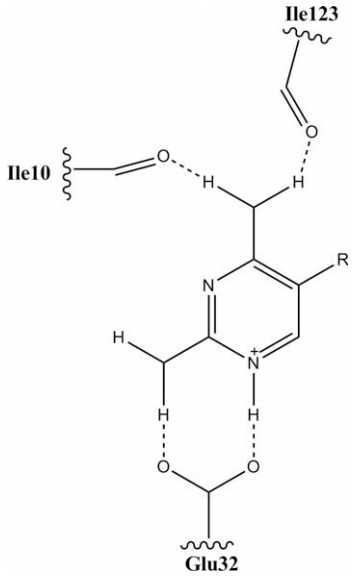

Figure 2. Experimentally observed conserved geometry in the active site of DHFR for compounds with a 2,4-diaminopyrimidine nucleus.

with the key active site residue Glu32, thereby rationalizing the low experimentally observed activity for this compound. The *s*-triazine ring in compounds, **3b–c**, (Fig. 3b and c) showed additional π–π stacking interaction with phenyl ring of Phe36 (centroid–centroid distance 4.1 Å for **3b** and 4.4 Å for **3c**) at the bottom of active site. However, in compound, **3b**–**c**, (Fig. 3b and c) the *s*-triazine ring was not orientated properly, possibly due to the presence of a one carbon bridge joining the tricyclic moiety and *s*-triazine ring system which is too short. Single hydrogen bonding interaction with Glu32 in, **3b–c**, could be the reason for better activity of these compounds compared to **3a**. However, the absence of the key bipolar interaction with Glu32 as depicted in Figure 2, at the bottom of active site was responsible for the low activity of, **3a–c**.

In contrast to the bulky *s*-triazine derivatives, in compounds **8a–b** (Fig. 3g), the 2,4-diaminopyrimidine ring orients properly in the active site. The 4-amino group in these compounds is involved in hydrogen bonding interaction with Ile123, while the

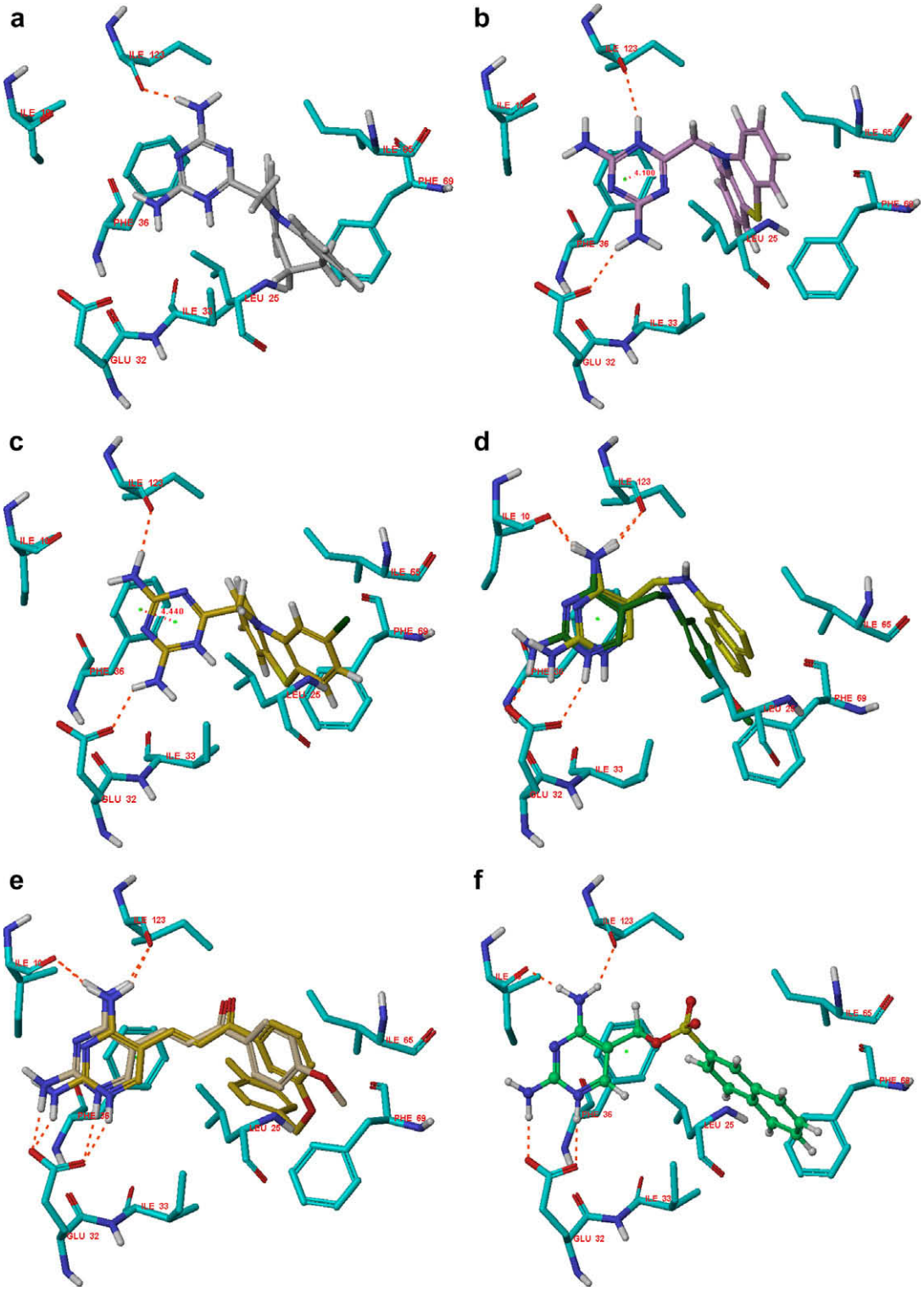

Figure 3. Predicted binding modes of the synthesized compounds in the active site of pcDHFR; (a) binding mode of compound **3a** (off white color); (b) binding mode of compound **3b** (plum color); (c) binding mode of compound **3c** (yellow color); (d) binding mode of compound **5a–b** (**5a**, green color; **5b**, yellow color); (e) binding mode of compound (**6a–b**); (f) binding mode of compound **7a** (green color); (g) binding mode of compound **8a–b** (**8a**, off plum color; **8b**, green color); (h) binding mode of compound **8c** (green color); (i) binding mode of compound **8d** (violet color); (j) binding mode of compounds **11a–b** (**11a**, violet color; **11b**, green color).

2-amino group is involved in hydrogen bonding interaction with Glu32, thereby making these compounds better inhibitors than **3a–c**. Furthermore, dihydrodibenz[*b,f*]azepine analog, **8b**, showed proper orientation of the tricyclic moiety in the active site.

Compounds, **5a–b** and **8c**, showed conserved interactions of 2,4-diaminopyrimidine ring system with Ile123, Ile10 and Glu32. The methyl group of *p*-OCH_3 substitution in compound, **5a**, (Fig. 3d) was involved in hydrophobic interaction with Phe69. In compound, **5b**, (Fig. 3d) the napthyl ring system showed additional

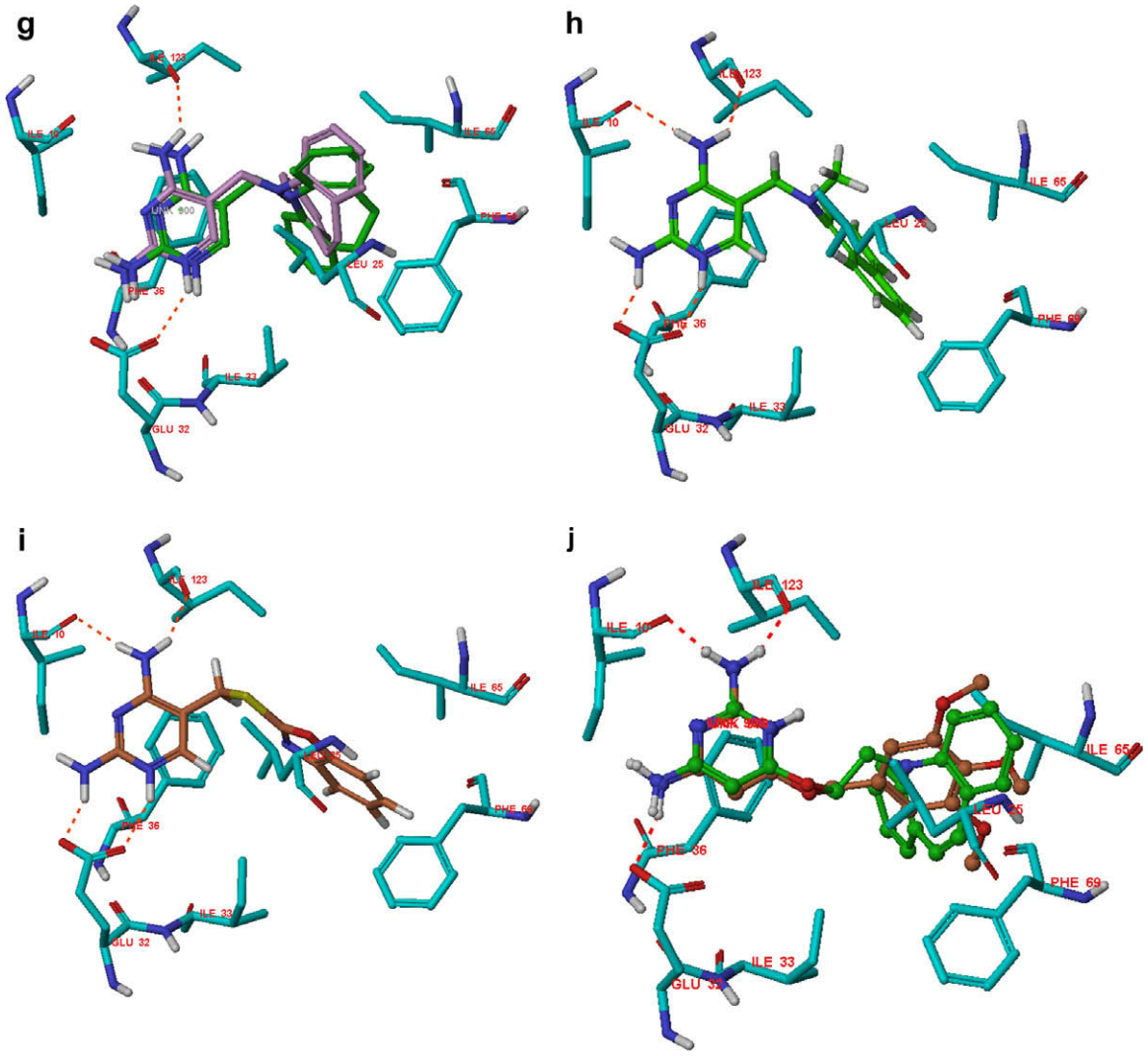

Fig. 3 (*continued*)

hydrophobic interactions with Leu32, Ile65, Phe69, Leu25 and Ile33 residues of the active site. No direct interactions were observed with the bridge; however it mainly affects the orientation of the distal ring. In compound, **8c**, (Fig. 3h) the methyl group on bridge showed hydrophobic interaction with Leu25, in addition, presence of this methyl group helps to orient the napthyl moiety deeper in the hydrophobic pocket which can be attributed to observed good activity of this compound.

The reason for inactivity of, **6a–b**, (Fig. 3e) could not be anticipated from the predicted binding modes as both compounds show conserved interactions with Ile123, Ile10 and Glu32, in addition, favorable hydrophobic interactions with the distal part were also seen. As mentioned previously, high conformational restriction could be the reason for inactivity of these compounds.

The extended electronegative bridges in compounds, **7a** (Fig. 3f) and **8d**, (Fig. 3i) possess both the 2,4-diaminopyrimidine and distal ring in correct orientation. In both compounds, 4-amino group showed hydrogen bonding interactions with Ile123 and Ile10. In particular, the 2-amino group and protonated N1 in both the compounds showed bipolar conserved interaction with Glu32 of active site which is essential requirement for DHFR inhibitory activity. The napthyl ring of compound, **7a**, showed good hydrophobic interactions with Leu32, Ile65, Phe69, Leu25 and Ile33, thus making this compound active and selective for pcDHFR.

Compounds, **11a–b**, (Fig. 3j) showed H-bonding interactions of 2,4-diaminopyrimidine ring system with Ile123, Ile10 and Glu32. However, key bipolar interaction with active site residue Glu32 was missing; this could be the reason for observed less activity. Furthermore, **11b**, forms several good hydrophobic interactions with Leu25, Ile33, Phe36, Ile65 and Phe69 which explains the better activity of **11b** over **11a**.

In order to predict the relative binding affinities of these compounds, Glide-XP scores and binding energy ΔG_{bind} values calculated using MM-GBSA protocol were compared with experimental IC_{50} values. This comparison of docking scores, ΔG_{bind} and IC_{50} values clearly shows that the relative binding affinities of two compounds, **6a–b**, were overestimated by both methods. Also, the experimental IC_{50} of compound, **11a**, was not exactly determined. Hence, these compounds were considered as outliers and were excluded from further regression analysis.

The predicted Glide-XP score values vary from −12.18 to −5.75 kcal/mol (Table 2). Glide-XP scores showed a fair correlation coefficient of 0.538 (Fig. 4) with the experimentally determined IC_{50} values. Interestingly, the most inactive ligand, **11a**, was also predicted to be lowest active using Glide-XP score. Furthermore, Glide-XP score was able to clearly distinguish between active and inactive ligands. For instance, all the compounds with good activity **7a**, **8a–d**, **I** and trimethoprim, scored higher than the low active

Table 2
Comparison of experimental binding energy with docking scores and MM-GBSA predicted binding affinities ΔG_{bind} against pcDHFR

Mol ID	pcDHFR activity IC_{50} (μM)	XP GScore[a]	Evdw[a]	Ecoul[a]	ΔG_{bind}
3a	1265.15	−6.29	−22.66	−2.92	−15.95
3b	235.46	−7.09	−34.29	−1.05	−34.95
3c	603.65	−7.26	−31.23	−2.26	−32.24
5a	363.26	−8.50	−24.51	−7.65	−37.77
5b	150.58	−9.62	−28.72	−6.82	−36.57
6a	151.319 (4)	−10.17	−31.97	−7.62	−43.02
6b	11.653 (2)	−11.83	−35.94	−5.77	−52.01
7a	7.88	−10.82	−32.72	−8.76	−45.08
8a	26.25	−11.34	−33.25	−4.44	−34.43
8b	0.84	−9.26	−29.61	−2.87	−38.23
8c	38.48	−11.02	−27.77	−6.14	−42.30
8d	35.83	−9.24	−26.09	−7.51	−36.26
11a	148.635 (0)	−5.48	−40.10	−7.19	−40.84
11b	112.02	−7.85	−29.90	−7.08	−42.36
TMP*	13.00	−10.15	−30.34	−7.42	−41.50
I*	0.21	−12.19	−42.74	−7.64	−45.39

* TMP is trimethoprim and I is depicted in Fig. 1.
[a] XP GScore is the predicted binding energy using Glide in kcal/mol; Evdw and Ecoul are the vdW and electrostatic interaction energies between ligand and receptor calculated using Glide-XP; ΔG_{bind} is predicted binding affinity using MM-GBSA.

compounds **3a–c** and **5a–b**. Inspection of Evdw and Ecoul terms which are van der Waals interaction energy and electrostatic interaction energy predicted by Glide-XP revealed that all ligands share higher values of van der Waals interaction energy which is logical considering the lipophilic distal part substitutions. Furthermore, a striking observation was that, for all most active compounds (except **8b**) the electrostatic interaction energy term is higher than the inactive compounds, which is in accordance with the conserved bipolar interaction with Glu32 at bottom of active site in the most active compounds.

In order to improve correlation between the observed IC_{50} values and predicted binding affinity, MM-GBSA post docking scoring protocol was employed. Concisely, various energy components which contribute to binding energy such as free energy, solvation energy and surface area energy were calculated for the complex holoenzyme, apoenzyme and free ligand; binding energy was calculated as the sum of difference between energy of complex holoenzyme and sum of energy of apoenzyme and free ligand. The results of binding affinity prediction using MM-GBSA are tabulated in Table 2. Interestingly, the MM-GBSA predicted binding energy ΔG_{bind} could clearly distinguish between active and inactive ligands. Also, improved correlation coefficient of 0.797 (Fig. 4) was obtained between IC_{50} values and predicted binding affinity.

To understand the electronic distribution of molecule in the active site the docked pose conformer of compound, **7a**, was subjected to single point energy calculation using density functional theory (DFT) B3LYP/3-21G* level of basis set. The calculated molecular electrostatic potential (MESP) map is depicted in Figure 5 on the scale of 10–225 kcal/mol. The most positive, deepest blue color colored regions by the hydrogen of both amino groups and hydrogen of protonated N1, are in accordance with the H-bonding with receptor active site. The least positive potential regions (deepest red color), were seen in the vicinity of oxygen of sulfonyl group.

3. Conclusion

Fourteen novel, diverse compounds with varying pharmacophoric features, bulky distal substitutions and different bridges were designed and synthesized as DHFR inhibitors. The synthesized compounds were evaluated against DHFR from opportunistic microorganisms using in vitro assays. Some of the synthesized compounds showed appreciable selective activity against DHFR from opportunistic microorganisms. In particular compound, **7a**, was found to be selective for pcDHFR with approximately twofold increase in activity and good selectivity when compared to trimethoprim. The observed experimental results were used to establish and understand binding modes of these compounds using molecular modeling studies. Thus, the present study provides not only novel scaffold for the further optimization of DHFR inhibitors but also an understanding the specific interactions of inhibitors with DHFR and structural modifications that improve selectivity.

4. Experimental

4.1. General considerations

Melting points were recorded on Thermomix Compbell electronics, having oil-heating system and were uncorrected. The microwave reactions were carried out using CEM Focused Microwave System in monomode, Model Discover. Analytical thin-layer chromatography (TLC) was carried out on precoated plates SiO_2 (Silica Gel 60, F 254, Merck). SiO_2 (Silica gel 420, Merck) was used for column chromatography using CombiFlash® RETRIEVE® system. FTIR spectra were recorded on 'Buck scientific infrared spectroscopy M500 spectrophotometer' using KBr pellets. NMR spectra were recorded on JEOL AL 300 MHz spectrometer or Bruker DMX-500 spectrometer operating at 500 MHz with DMSO-d_6 as solvent; s = singlet, d = doublet, t = triplet, q = quartet, m = mutiplet, br = broad. The mass spectrum was recorded on a Waters Q/TOF Micromass spectrometer. All the reagents and chemicals used were of 'reagent grade'.

4.2. Chemistry

4.2.1. 6-((10,11-Dihydro-5*H*-dibenzo[*b*,*f*]azepin-5-yl)methyl)-1,3,5-triazine-2,4-diamine (3a)

A solution of **1a** (1 g, 0.0051 mol), K_2CO_3 (0.71 g, 0.0051 mol), PEG 6000 (125 mg, 12.5% w/w), water (1 ml) in chloroacetonitrile (5 ml) was heated at 150 °C for 24 h. Column purification of the

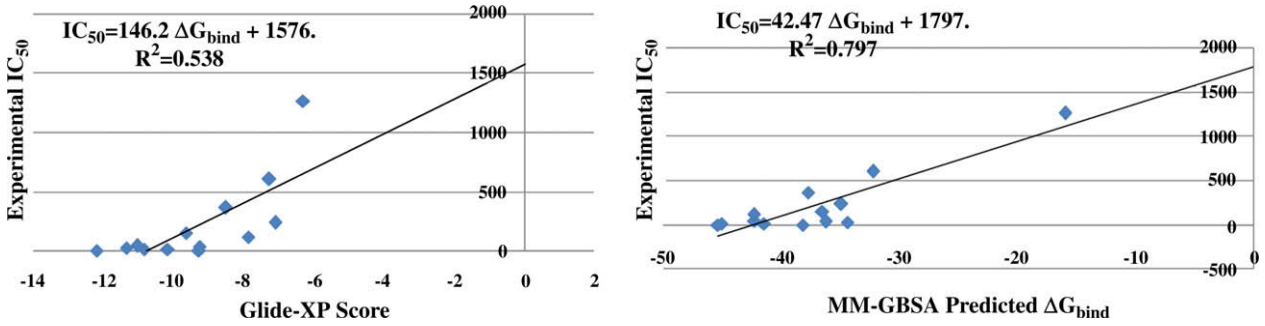

Figure 4. Correlation between Glide-XP scores, MM-GBSA predicted binding affinities and experimentally determined IC_{50} values against pcDHFR.

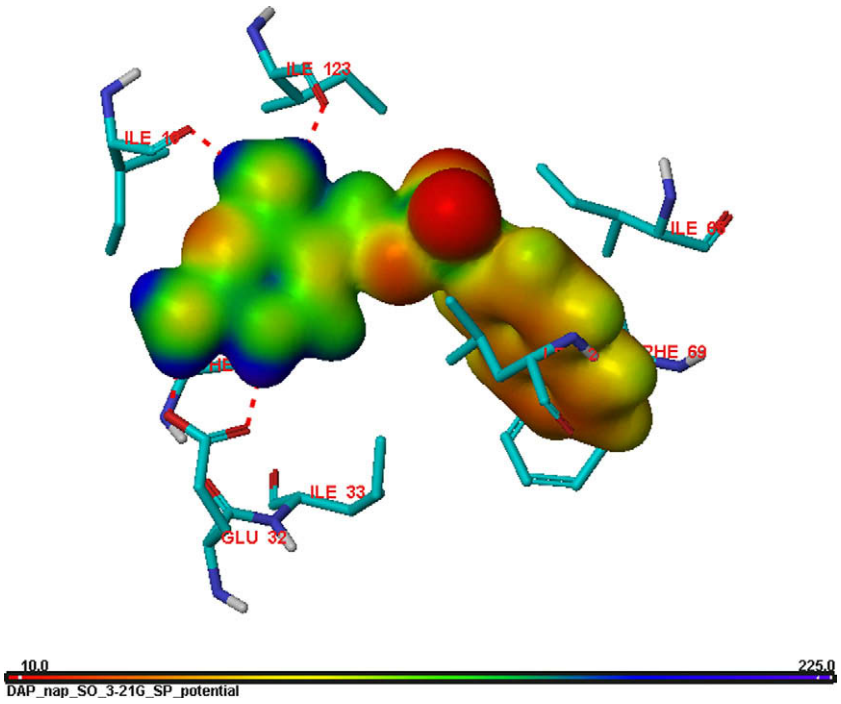

Figure 5. MESP superimposed onto a surface of constant electron density (0.01 e/au^3) for compound, **7a**, showing the most positive potential region (deepest blue color) by hydrogen of both amino groups and hydrogen of protonated N1 and the least positive potential regions (deepest red color) were seen in the vicinity of oxygen of sulfonyl group.

reaction mixture yielded 0.38 g (31.7%) of **2a**.[11] Compound **2a** (0.38 g, 0.00162 mol), dicyandiamide (0.15 g, 0.0017 mol), was stirred in 2-methoxyethanol (10 ml) in presence of KOH (0.25 g) and water (0.2 ml). The resultant reaction mixture was subjected to microwave irradiation at a power of 100 for 20 min to attain the target temperature of 150 °C. TLC monitoring showed formation of product along with the unreacted starting material. The reaction mixture was poured into cold water resulting in solid precipitate. Filtration followed by washings with hot water (2 × 20 ml) and with 20% EtOAc/*n*-hexanes mixture to remove unreacted **2a**, yielded 0.046 g (yield: 9%) of 6-((10,11-dihydro-5*H*-dibenzo[*b*,*f*]azepin-5-yl)methyl)-1,3,5-triazine-2,4-diamine (**3a**, Scheme 1) as brown solid. Mp = 227 °C. IR (KBr) V_{max} cm^{-1} 3463, 3297, 3178, 3102, 1616, 1565, 1543, 1506, 1486, 1453, 1384, 1233; ^{1}H NMR (DMSO-d_6, 300 MHz): δ 7.15–7.04 (m, 6H, Ar–H), 6.86–6.82 (t, 2H, Ar–H), 6.58 (s, 4H, D_2O exchangeable –NH_2), 4.56 (s, 2H, –CH_2), 3.11 (s, 4H, ring –CH_2–CH_2–, overlapped with H_2O peak of DMSO-d_6); ^{13}C NMR (DMSO-d_6, 75 MHz): δ 167.0, 167.0, 167.0, 147.8, 133.4, 129.5, 126.1, 121.8, 120.2, 58.6, 32.4; *M*/*S* 319.33 [M+1]$^+$.

4.2.2. 6-((10*H*-Phenothiazin-10-yl)methyl)-1,3,5-triazine-2,4-diamine (3b)

NaH (0.22 g, 0.0050 mol) was added to a solution of **1b** (1 g, 0.0050 mol) in dry DMF (5 ml) and reaction mixture was stirred at room temperature for 20 min. Chloroacetonitrile (0.38 g, 0.0050 mol) was added and reaction mixture was heated on a water bath at 60–80 °C for 3 h followed by stirring at room temperature for 12 h. Column chromatography yielded 0.47 g, (yield: 40%), pale white solid of **2b**.[11] The solution of **2b** (0.2 g, 0.00084 mol) in methoxyethanol (10 ml) was treated with dicyandiamide (0.071 g, 0.00084 mol), KOH (0.2 g) and water (0.2 ml).[13] The resultant reaction mixture was heated at 100 °C for 12 h. Column chromatography yielded 0.139 g (yield: 51.48%) of 6-((10*H*-phenothi azin-10-yl)-methyl)-1,3,5-triazine-2,4-diamine (**3b**, Scheme 1) as dark green solid. Mp = 226–228 °C; IR (KBr) V_{max} cm^{-1} 3460, 3218, 2911, 1647, 1599, 1460, 1394, 1247, 1212, 1097; ^{1}H NMR (DMSO-d_6, 300 MHz): δ 7.73 (s, 1H, D_2O exchangeable –NH_2), 7.34 (s, 1H, D_2O exchangeable –NH_2), 7.16–7.07 (m, 3H, Ar–H; 1H, D_2O exchangeable –NH_2), 6.97–6.90 (m, 3H, Ar–H; 1H, D_2O exchangeable –NH_2), 6.68 (s, 3H, Ar–H), (s, 2H, –CH_2); ^{13}C NMR (DMSO-d_6,75 MHz): δ 169.9, 169.9, 169.8, 145.7, 143.6, 131.9, 127.6, 127.4, 126.5, 123.1, 122.0, 121.0, 120.4, 115.4, 115.1, 50.9; *M*/*S* 321.28 [M−1]$^+$.

4.2.3. 6-((2-Chloro-10*H*-phenothiazin-10-yl)methyl)-1,3,5-triazine-2,4-diamine (3c)

NaH (0.28 g, 0.0064 mol) was added to a solution of **1c** (Scheme 1) (1 g, 0.0043 mol) in dry DMF (5 ml) and reaction mixture was stirred at room temperature for 20 min. Chloroacetonitrile (0.32 g, 0.0043 mol) was added and reaction mixture was heated on water bath at 60–80 °C for 3 h, followed by stirring at room temperature for 12 h. Column chromatography led to 0.20 g, (yield: 17.15%), whitish pink solid of **2c**.[12] The solution of **2c** (0.2 g, 0.00073 mol) in methoxyethanol (10 ml) was treated with dicyandiamide (62 mg, 0.00073 mol), KOH (0.2 g) and water (0.2 ml). The resultant reaction mixture was heated at 100 °C for 12 h. Column chromatography yielded 0.039 g (yield: 25%) of 6-((2-chloro-10*H*-phenothiazin-10-yl)methyl)-1,3,5-triazine-2,4-diamine (**3c**, Scheme 1) as dark green solid. Mp = 197 °C; IR V_{max} cm^{-1} 3467, 3307, 3100, 1652, 1627, 1559, 1544, 1312, 1255, 1209, 803; ^{1}H NMR (DMSO-d_6, 300 MHz): δ 7.03–7.01 (m, 3H, Ar–H; 1H, D_2O exchangeable –NH_2), 6.91 (2H, Ar–H; 1H, D_2O exchangeable –NH_2), 6.75–6.65 (2H, Ar–H; 2H, D_2O exchangeable –NH_2), 4.65 (s, 2H, –CH_2); ^{13}C NMR (DMSO-d_6, 75 MHz): δ 173.8, 166.9, 145.5, 143.4, 131.9, 127.6, 127.1, 126.2, 122.8, 121.8, 120.5, 120.0, 116.0, 115.9, 115.5, 53.8; *M*/*S* 357.24 [M+1]$^+$, 359.19.

4.2.4. 2,4-Diaminopyrimidine-5-carbonitrile (5, Scheme 2)[14–17]

To the freshly prepared sodium ethoxide (sodium (1.0 g, 0.0438 mol) in 20 ml absolute ethanol) solution; guanidine nitrate **4**, was added (5 g, 0.0409 mol) and the reaction mixture was heated to reflux for 10–15 min, the clear solution immediately

turned turbid white. The solution was filtered and washed with 10 ml absolute ethanol and the filtrate with combined washings was used further. To the filtrate, ethoxymethylene malononitrile (5 g, 0.049 mol) was added in portions for 15–20 min and the reaction mixture was cooled to 10 °C and stirred for 8 h, after which it was concentrated to dryness and the obtained residue was dissolved in glacial acetic acid and then given charcoal treatment. The reaction mixture was filtered and the charcoal cake was washed with 10 ml glacial acetic acid. The filtrate and washings were collected together and cooled to 10 °C. On cooling yellow crystals started precipitating out. To the cooled filtrate, 30% ammonium hydroxide solution was added till it became neutral, which led to further precipitation of solid product. The product was filtered, washed with copious amount of cold water and then dried to yield 3.5 g, (yield: 63%) of 2,4-diaminopyrimidine-5-carbonitrile (**5**, Scheme 2) as yellow solid: mp = 318 °C, lit.[14] mp = 317 °C; IR (KBr) V_{max} cm^{-1} 3430, 3336, 3104, 2202, 1652, 1586, 1548, 1475, 1354, 1282 cm^{-1}; ^1H NMR (DMSO-d_6, 500 MHz): δ 8.18 (s, 1H, –CH), 6.80–7.10 (br s, 4H, D_2O exchangeable $-NH_2$); *M*/*S* 136.04 $[M+1]^+$.

4.2.5. 2,4-Diaminopyrimidine-5-carbaldehyde (6, Scheme 2)[14–17]

Raney nickel (2.5 g of 50% slurry with water) was added to a solution of **5**, (2.25 g, 0.0166 mol) in 98–100% formic acid (20 ml) and the reaction mixture was refluxed for 3–4 h. After which, the reaction mixture was filtered and washed with 10 ml formic acid. The filtrate and washings were collected together and concentrated under reduced pressure. The resulting residue was stirred in 30% ammonia solution and cooled to get free flowing solid product which was filtered and washed with water followed by drying to get 1.8 g, (yield: 78.29%) of 2,4-diaminopyrimidine-5-carbaldehyde (**6**, Scheme 2) as off white solid. Mp = chars at 270–272 °C; IR (KBr) V_{max} cm^{-1} 3424, 3384, 3142, 1635, 1594, 1506, 1407, 1236; ^1H NMR (DMSO-d_6, 500 MHz): δ 9.42 (s, 1H, –CHO), 8.25 (s, –1H, –Het Ar–H), 7.59–7.80 (d, 2H, D_2O exchangeable $-NH_2$), 7.20 (s, 2H, D_2O exchangeable $-NH_2$); *M*/*S* 139.03 $[M+1]^+$.

4.2.6. (2,4-Diaminopyrimidin-5-yl)methanol (7, Scheme 2)[14–17]

$NaBH_4$ (0.41 g, 0.0108 mol) was added to a methanolic solution of **6**, (1 g, 0.0072 mol) and reaction mixture was stirred at room temperature for 4–5 h. After which the clear reaction mixture was concentrated to dryness and obtained pale white pasty mass was stirred in 3 ml of cold water and refrigerated for 12 h to obtain free flowing solid product. The solid obtained was filtered and washed with 2 ml cold water, dried to get 0.56 g, (yield: 55.4%) of (2,4-diaminopyrimidin-5-yl)methanol (**7**, Scheme 2) as greenish yellow solid. decomposes at 263–265 °C, lit.[14] = decomposes at 265 °C; *M*/*S* 141.1 $[M+1]^+$.

4.2.7. 5-(Bromomethyl)pyrimidine-2,4-diamine (8, Scheme 2)[18]

Compound **7** (0.2 g, 0.0014 mol) was dissolved in glacial acetic acid (4 ml) by heating the reaction mixture at 40–50 °C. This lemon yellow solution was cooled gradually to room temperature (in case solid started precipitating out, 1–2 ml more of glacial acetic acid was added to get a clear solution). To the clear solution, 3 ml of 30–32% HBr in acetic acid was added drop wise over a period of 20 min. Solid precipitation was observed within addition of first few drops of HBr solution, which disappeared on addition of more HBr solution. After completion of addition of HBr solution, reaction mixture was heated at 60 °C for 2–3 h till TLC showed completion of reaction. The reaction mixture was then concentrated to dryness by azeotropic distillation using toluene under reduced pressure at 50–55 °C. The product obtained as hydrobromide salt being very unstable was used as such without further purification.

4.2.8. 5-((4-Methoxyphenylamino)methyl)pyrimidine-2,4-diamine (5a)

Raney nickel (1 g) and *p*-anisidine (0.2 g, 0.0017 mol) were added to a solution of **5** (0.2 g, 0.00148) in glacial acetic acid (20 ml) at room temperature. The resultant reaction mixture was stirred for 2–6 h under H_2 atmosphere.[19] After completion of the reaction (monitored by TLC) the reaction mixture was filtered, washed with glacial acetic acid (10 ml). The filtrate and washings were collected together and concentrated azeotropically using toluene to dryness under reduced pressure at 50–55 °C. The obtained slurry was treated with 1 N Na_2CO_3 to get free flowing solid. The resultant mixture was cooled, filtered and washed with water till the washings were neutral to pH paper. Solid was then washed with 20% EtOAc/*n*-hexanes solution to remove any non-polar impurity. The solid thus obtained was dried in oven to get 0.28 g, 71.79% brownish yellow solid. Mp = 215–217 °C; IR (KBr) V_{max} cm^{-1} 3420, 3212, 2952, 2835, 2929, 1683, 1602, 1527, 1501, 1460, 1286, 1246, 1206, 1178, 1108, 1030; ^1H NMR (DMSO-d_6, 300 MHz): δ 8.76- 8.13 (m, 2H, Ar–H; 1H, –NH, D_2O exchangeable), 7.15–6.63 (m, 4H, Ar–H; 2H, –NH, D_2O exchangeable), 3.69 (s, 3H, $-OCH_3$, overlapped with H_2O peak of DMSO-d_6); ^{13}C NMR (DMSO-d_6, 75 MHz): 162.6, 162.6, 161.8, 157.2, 144.1, 127.8, 121.8, 114.8, 114.3, 103.5, 55.1, 43.8; *M*/*S* 244.21 $[M-1]^+$, 245.28.

4.2.9. 5-((Naphthalen-1-ylamino)methyl)pyrimidine-2,4-diamine (5b)

Raney nickel (1 g), 1-napthyl amine (0.25 g, 0.00178 mol), 2,4-diaminopyrimidine-5-carbonitrile (0.2 g, 0.00148 mol) were used following the same procedure as described for **5a**, to yield 0.28 g, 77.77% greenish yellow solid. Mp = 214 °C; IR (KBr) V_{max} cm^{-1} 3365, 3310, 3133, 1659, 1616, 1565, 1529, 1500, 1451, 1394, 1245 cm^{-1}; ^1H NMR (DMSO-d_6, 300 MHz): δ 8.86 (br s, 1H, –NH D_2O exchangeable), 8.48 (s, 1H, Ar–H), 8.23–8.17 (m, 2H, Ar–H), 7.92–7.90 (s, 1H, –NH), 7.74–7.71 (d, 1H, Ar–H), 7.52–7.47 (m, 3H, Ar–H), 7.17–7.14 (d, 1H, Ar–H), 6.76 (s, 2H, –NH D_2O exchangeable) (Bridge –CH2 peak got overlapped with H_2O peak of DMSO-d_6); ^{13}C NMR (DMSO-d_6, 75 MHz): δ 163.6, 163.1, 162.1, 159.7, 148.5, 133.6, 128.1, 127.8, 126.4, 125.8, 124.7, 123.0, 113.2, 103.7, 40.3; *M*/*S* 264.04 $[M-1]^+$.

4.2.10. 3-(2,4-Diaminopyrimidin-5-yl)-1-(4-methoxyphenyl)-prop-2-en-1-one (6a)

0.5 ml of 10% NaOH solution was added to a solution of *p*-methoxyacetophenone (0.1 g, 0.00072 mol) in 5 ml DMSO and the reaction mixture was stirred at 40–50 °C for 60 min followed by addition of **6** (0.1 g, 0.00072 mol). The resultant reaction mixture was stirred at 40–50 °C for 8 h. TLC monitoring showed product spot along with the spot of unreacted *p*-methoxyacetophene. The reaction mixture was poured to the cold water. The precipitated solid was filtered and washed with water till the filtrate was neutral to pH paper. The solid obtained was purified by column chromatography to yield 29 mg, (15% yield) of pure product as bright yellow solid. Mp = chars at 198 °C; IR V_{max} cm^{-1} 3115, 2956, 1668, 1595, 1541, 1472, 1322, 1249, 1173; ^1H NMR (DMSO-d_6, 300 MHz): δ 9.09 (s, 1H, CH=CH), 8.20–8.18 (d, 2H, Ar–H, 1H, –NH D_2O exchangeable), 7.79–7.77 (s, 1H, Ar–H), 7.79–7.77 (d, 1H, –CH=CH), 7.08 (m, 3H, Ar–H; 1H, 1H, –CH=CH; 2H, –NH D_2O exchangeable), 3.81 (s, 3H, $-OCH_3$); ^{13}C NMR (DMSO-d_6, 75 MHz): δ 163.6, 163.4, 162.4, 161.4, 138.0, 130.7, 129.3, 114.8, 114.4, 55.5; *M*/*S* 271.22 $[M+1]^+$.

4.2.11. 3-(2,4-Diaminophenyl)-1-(3-(4-methylbenzyloxy)phenyl)prop-2-en-1-one (6b)

1-(3-(4-Methylbenzyloxy)phenyl)ethanone (0.2 g, 0.0015 mol), **6** (0.2 g, 0.0015 mol) were used following the same procedure as described for **6a**, to yield 94 mg, (18% yield) of pure product as yel-

lowish-brown solid. Mp = chars at 218 °C; IR V_{max} cm^{-1} 3413, 3320, 3123, 2916, 1654, 1606, 1545, 1466, 1193, 1018; ^1H NMR (DMSO-d_6, 300 MHz): δ 9.15 (s, 1H, CH═CH), 8.28–8.26 (d, 1H, CH═CH); 7.86 (m, 3H, Ar–H), 7.43–7.35 (m, 3H, Ar–H; 1H, –NH D_2O exchangeable), 7.21–7.18 (m, 3H, Ar–H; 3H, 2H, –NH D_2O exchangeable), 5.15 (s, 2H, $-CH_2$), 2.29 (s, 3H, $-CH_3$); ^{13}C NMR (DMSO-d_6, 75 MHz): δ 163.5, 162.2, 159.7, 158.8, 158.8, 139.7, 138.0, 137.0, 133.9, 129.0, 127.8, 120.0, 117.1, 115.2, 113.4, 112.6, 69.2, 20.7; *M*/*S* 359.2 $[M+1]^+$.

4.2.12. (2,4-Diaminopyrimidin-5-yl)methyl naphthalene-2-sulfonate (7a)

Naphthalene-2-sulfonyl chloride (0.32 g, 0.00143 mol) was added to a solution of **7** (0.2 g, 0.00143 mol) in 1 ml DMSO and triethylamine (0.144 g, 0.00143 mol) and the reaction mixture was stirred at room temperature for 8 h. After completion of reaction (monitored by TLC), reaction mixture was added to water and extracted with 80% chloroform/methanol mixture. Column purification gave 70 mg (yield 15%) of product as white solid. Mp 195–196 °C; IR (KBr) V_{max} cm^{-1} 3342, 1656, 1544, 1483, 1270, 1174, 1122, 1070; ^1H NMR (DMSO-d_6, 300 MHz): δ 8.74 (s, 1H, Ar–H), 8.21–8.14 (m, 2H, Ar–H), 7.99–7.72 (m, 3H, Ar–H; 2H, –NH D_2O exchangeable), 7.69–7.52 (m, 2H, Ar–H; 2H, –NH D_2O exchangeable), 4.17 (s, 2H, $-CH_2$ overlapped with H_2O peak of DMSO-d_6); ^{13}C NMR (DMSO-d_6, 75 MHz): δ 162.5, 162.4, 152.0, 140.1, 133.9, 132.7, 131.6, 129.2, 127.4, 126.4, 124.0, 109.8, 56.4; *M*/*S* 331.43 $[M+1]^+$.

4.2.13. 5-((5*H*-Dibenzo[*b*,*f*]azepin-5-yl)methyl)pyrimidine-2,4-diamine (8a)

NaH (50 mg, 0.011 mol) was added to a solution of iminostilbene (0.18 g, 0.00093 mol) in 5 ml dry THF and the reaction mixture was stirred at room temperature under N_2 atmosphere for 2 h. To this reaction mixture freshly prepared hydrobromide salt of 5-(bromomethyl) pyrimidine-2,4-diamine **8**, dissolved in dry *N*,*N*-dimethylacetamide (15 ml) was added and the resultant reaction mixture was stirred at room temperature for three days.[3,5] TLC monitoring showed formation of new spots along with unreacted iminostilbene. Column purification of the crude product yielded 60 mg, 20.5%, greenish yellow solid. Mp = 116–117 °C; IR (KBr) V_{max} cm^{-1} 3341, 3185, 3019, 3061, 2926, 2853, 1659, 1607, 1487, 1456, 1425, 1290, 761; ^1H NMR (DMSO-d_6, 300 MHz): δ 7.75 (s, 1H, Ar–H), 7.30–6.97 (m, 8H, Ar–H), 6.82 (s, 2H, –CH═CH), 6.20 (s, 2H, –NH D_2O exchangeable), 5.73 (s, 2H, –NH D_2O exchangeable), 4.61 (s, 2H, $-CH_2$); ^{13}C NMR (DMSO-d_6, 75 MHz): 162.9, 162.3, 156.7, 149.3, 133.1, 131.8, 128.8, 123.6, 120.7, 101.5, 48.9; *M*/*S*: 316.04 $[M+1]^+$.

4.2.14. 5-((10,11-dihydro-5H-dibenzo[*b*,*f*]azepin-5-yl)methyl)-pyrimidine-2,4-diamine (8b)

NaH (55 mg, 0.00125mol), dihydroiminostilbene (0.25g, 0.00128 mol) were used following the same procedure as described for **8a**, to yield 26 mg, 6.4%, greenish yellow solid. Mp = 105 °C; IR (KBr) V_{max} cm^{-1} 3320, 3185, 2926, 1648, 1601, 1524, 1492, 1342, 756; ^1H NMR (DMSO-d_6, 300 MHz): δ 8.25 (s, 2H, –NH D_2O exchangeable), 7.69–6.63 (8H, Ar–H; 4H, –NH D_2O exchangeable), 3.52 (s, 2H, –CH, overlapped with DMSO peak), 2.92 (s, 4H, –CH); *M*/*S*: 318.50 $[M+1]^+$.

4.2.15. 5-((Methyl(naphthalen-1-yl)amino)methyl)pyrimidine-2,4-diamine (8c)

The solution of 1-napthylamine (2 g, 0.0139 mol), methyl iodide (2.18 g, 0.0139 mol) and K_2CO_3 (2.31 g, 0.0167 mol) in acetonitrile (30 ml) was stirred at 40–50 °C in dark for three days. TLC showed two spots along with unreacted 1-napthylamine spot. Reaction mixture was purified by column chromatography to yield 0.33 g, 15% of *N*-methylnaphthalen-1-amine[19] which was dissolved in 5 ml dry THF at room temperature under N_2 atmosphere for 5 min. To this clear solution NaH (92 mg, 0.00210 mol) was added and the resultant reaction mixture was stirred at room temperature under N_2 atmosphere for 2 h. To this reaction mixture freshly prepared hydrobromide salt of **8**, dissolved in dry *N*,*N*-dimethylacetamide (15 ml) was added and the resultant reaction mixture was stirred at room temperature for three days. TLC monitoring showed formation of new spot along with unreacted starting material. Column purification gave 110 mg, 19%, off white solid. Mp = 221 °C; IR (KBr) V_{max} cm^{-1} 3363, 2936, 1638, 1498, 1399, 1223, 761; ^1H NMR (DMSO-d_6, 300 MHz): δ 8.36–8.29 (m, 2H, Ar–H), 8.08 (s, 1H, Ar–H), 7.83–7.08 (m, 4H, Ar–H; 4H, –NH D_2O exchangeable), 6.86–6.77 (d, 1H, Ar–H), 3.12 (s, 3H, $-CH_3$): ^{13}C NMR (DMSO-d_6, 75 MHz): 164.2, 154.5, 139.7, 138.9, 131.4, 128.4, 128.3, 127.9, 126.8, 126.4, 124.8, 124.2, 119.7, 107.9, 48.7; *M*/*S*: 280.10 $[M+1]^+$.

4.2.16. 5-((Benzo[*d*]oxazol-2-ylthio)methyl)pyrimidine-2,4-diamine (8d)

NaH (62 mg, 0.00141mol) was added to a solution of 2-mercaptobenzoxazole (0.21 g, 0.00139 mol) in 5 ml dry THF under the N_2 atmosphere. Freshly prepared hydrobromide salt of **8**, dissolved in dry *N*,*N*-dimethylacetamide (15 ml) was added and the resultant reaction mixture was stirred at room temperature for three days. TLC monitoring showed formation of new spots along with unreacted 2-mercaptobenzoxazole, at this stage reaction mixture was purified using column chromatography, to yield 110 mg, 29%, off white solid. Mp = 124–126 °C; IR (KBr) V_{max} cm^{-1} 3346, 3187, 1683, 1532, 1505, 1456, 1256, 1236, 1212, 1133; ^1H NMR (DMSO-d_6, 300 MHz): δ 7.83 (s, 1H, Ar–H), 7.63 (2H, Ar–H;), 7.31 (s, 2H, –Ar–H), 6.58 (s, 2H, –NH D_2O exchangeable), 5.98 (s, 2H, –NH D_2O exchangeable), 4.34 (s, 2H, –CH, overlapped with H_2O peak of DMSO-d_6); ^{13}C NMR (75 MHz): 172.1, 162.8, 162.0, 157.0, 151.1, 141.2, 124.6, 124.2, 118.2, 110.1, 100.6. 30.8; *M*/*S*: 274.33 $[M+1]^+$.

4.2.17. 6-(3,4,5-Trimethoxybenzyloxy)pyrimidine-2,4-diamine (11a)

NaH (0.20 g, 0.0086 mol) was added to a solution of **9** (1 g, 0.0069 mol) and **10a** (1.37 g, 0.0069 mol), in dry DMSO (5 ml) and reaction mixture was heated at 100 °C for 5–6 h. TLC monitoring showed formation of new spot along with unreacted starting material. Column purification yielded 1.22 g, (yield: 57%), white solid of **11a** (Scheme 3). Mp = 166–168 °C; ^1H NMR (DMSO-d_6, 300 MHz): δ 6.71 (s, 2H, Ar–H), 6.04–5.93 (d, 4H, D_2O exchangeable $-NH_2$), 5.09 (s, 3H, Ar–H; $-CH_2$), 3.75 (s, 6H, two $-OCH_3$), 3.63 (s, 3H, $-OCH_3$), ^{13}C NMR (DMSO-d_6,75 MHz): δ169.7, 166.0, 162.8, 152.7, 136.9, 133.0, 105.4, 76.2, 66.2, 59.9, 55.8; *M*/*S* 307.04 $[M+1]^+$.

4.2.18. 6-(2-(5*H*-Dibenzo[*b*,*f*]azepin-5-yl)ethoxy)pyrimidine-2,4-diamine (11b)

NaH (0.20 g, 0.0086 mol) was added to a solution of **9** (1 g, 0.0069 mol) and **10b** (1.64 g, 0.0069 mol), in dry DMSO (5 ml) wersxe used following the same procedure as described for **10a**, to yield 0.9 g, 37.8%, white solid **11b** (Scheme 3). Mp = 122–124 °C; ^1H NMR (DMSO-d_6, 300 MHz): δ 7.3–7.0 (m, 8H, Ar–H), 6.7 (s, 2H, Ar–H), 5.97–5.82 (d, 4H, D_2O exchangeable $-NH_2$), 4.97 (s, 1H, Ar–H), 4.09–4.00 (d, 4H, –CH═CH–), ^{13}C NMR (DMSO-d_6,75 MHz): δ 165.9, 165.8, 162.8, 150.2, 133.3,131.9, 129.1, 129.0, 123.4, 120.3, 76.1, 62.1, 49.0 *M*/*S* 346.07 $[M+1]^+$.

4.3. Biological assay

The synthesized compounds were evaluated for their ability to inhibit DHFR from pc, tg, ma and rl using a continuous spectropho-

tometric assay measuring oxidation at 340 nM of NADPH at 37 °C under conditions of saturating substrate and cofactor as previously described.[20,21]

4.4. Computational studies

4.4.1. Molecular docking

Docking studies were carried out using standard Glide molecular docking protocol implemented within Maestro molecular modeling suit by Schrödinger, LLC, New York, NY, 2008 installed on Intel Pentium 4 computer.[22]

The protein structure PDB code: 1KLK[4] which is the ternary complex of enzyme, NADPH and **I** (Fig. 1) with resolution of 2.3 Å was retrieved from Protein Data Bank (www.rcsb.com) and used for docking simulations. All water molecules were deleted, bond orders and charges of cofactor NADPH and 6-((5*H*-dibenzo[*b*,*f*]azepin-5-yl)methyl)pteridine-2,4-diamine, **I** (Fig. 1), were assigned properly in the protein preparation step, nitrogen N1 of inhibitor was protonated and given a +ve charge. A grid which is the representation of shape and properties of receptor using several different sets of fields was generated. The structure of **I** (Fig. 1) was randomized using Ligprep[23] and used for the cognate docking studies. The docking study was carried out using extra precision (XP) mode with 'must match' of at least one hydrogen bond criteria; with Ile123, Ile10 and Glu32 as these are the conserved residues in most of the DHFRs and H-bonding with these residues is one of the essential criteria for antifolate activity.

The structures of all synthesized compounds were constructed using MarvinSketch version 5.2 from ChemAxon Ltd[24] nitrogen N1 of all compounds was protonated and given a +ve charge. A unique low-energy 3D, protonated structure was generated for each ligand with the help of Ligprep,[23] where appropriate hydrogens were added to all structures and were subsequently subjected to energy minimization using the OPLS-2005 force field with a constant dielectric of 1.0. All ligands were docked using same protocol as described for compound **I**.

4.4.2. Binding affinity prediction using MM-GBSA

The assessment of molecular docking was carried out using a post scoring approach, MM-GBSA.[25] Maximum of top five docked poses returned using Glide-XP score were minimized using the local optimization feature[26] in Prime, and the energies were calculated using the OPLS-AA force field[27] and the GBSA continuum model.[27] For each molecule the best scoring pose predicted by MM-GBSA was selected for comparison with the experimental IC_{50} values. The binding free energy ΔG_{bind} was estimated as

$$\Delta G_{bind} = \Delta E_{MM} + \Delta G_{solv} + \Delta G_{SA}$$

where ΔE_{MM} is the difference in energy calculated using OPLS force field between the complexed holoenzyme structure and the sum of the energies of the ligand and apoenzyme, ΔG_{solv} is the difference in the GBSA solvation energy of the complexed holoenzyme and the sum of the solvation energies for the ligand and apoenzyme protein, and ΔG_{SA} is the difference in the surface area energy for the complexed holoenzyme and the sum of the surface area energies for the ligand and apoenzyme. Corrections for entropic changes were not applied.

4.4.3. MESP calculations

MESP computation was carried out using Jagur,[28] version 7.5, Schrödinger, LLC, New York, NY, 2008 installed on Intel Pentium 4 workstation using single point energy calculation at hybrid density functional theory with Becke's three-parameter exchange potential and the Lee-Yang-Parr correlation functional (B3LYP), using basis set 3-21G* level on the docked pose of **7a**.

Acknowledgments

Seema Bag is thankful to University Grand Commission (UGC), India and Nilesh R. Tawari is thankful to Department of Biotechnology (DBT), India for financial support.

Supplementary data

Supplementary data (^{1}H NMR and ^{13}C NMR spectra of all target molecules) associated with this article can be found, in the online version, at doi:10.1016/j.bmc.2010.03.031.

References and notes

1. Gangjee, A.; Yang, J.; Queener, S. F. *Bioorg. Med. Chem.* **2006**, *14*, 8341.
2. Klepser, M. E.; Klepser, T. B. *Drugs* **1997**, *53*, 40.
3. Rosowsky, A.; Cody, V.; Galitsky, N.; Fu, H.; Papoulis, A. T.; Queener, S. F. *J. Med. Chem.* **1999**, *42*, 4853.
4. Cody, V.; Galitsky, N.; Luft, J. R.; Pangborn, W.; Rosowsky, A.; Queener, S. F. *Acta Crystallogr., Sect. D* **2002**, *58*, 946.
5. Rosowsky, A.; Fu, H.; Queener, S. F. *J. Heterocycl. Chem.* **2000**, *37*, 921.
6. Rosowsky, A.; Fu, H.; Chan, D. C. M.; Queener, S. F. *J. Med. Chem.* **2004**, *47*, 2475.
7. Graffner-Nordberg, M.; Kolmodin, K.; Åqvist, J.; Queener, S. F.; Hallberg, A. *Eur. J. Pharm. Sci.* **2004**, *22*, 43.
8. Bag, S.; Tawari, N. R.; Degani, M. S. *QSAR Comb. Sci.* **2009**, *28*, 296.
9. Bag, S.; Tawari, N. R.; Queener, S. F.;. Degani, M. S., *J. Enzyme Inhib. Med. Chem.*, in press. doi: 10.3109/14756360903179443.
10. Degani, M. S. Bag, S.; Bairwa, R.; Tawari, N. R.; Queener, S. F., *J. Heterocycl. Chem.*, in press. doi: 10.1002/jhet.216.
11. Gabriele, B. A. *Process for Preparation of Opiramol. EP1 468* **2007**, *992*, B1.
12. Reddy, G. O.; Sarma, M. R.; Chandrasekhar, B.; Charan, C. J. A Process for the Preparation of 2-[Phenothiazin-10-yl] Ethyl methane sulfonate, WO 02/40460, 2002.
13. Simons, J. K.; Saxton, M. R. *Org. Synth.* **1963**, *Collective Vol. 4*, 78.
14. Huber, W. *J. Am. Chem. Soc.* **1943**, *65*, 2222.
15. Gangjee, A.; Adair, O. O.; Queener, S. F. *J. Med. Chem.* **2003**, *46*, 5074.
16. Wyss, P. C.; Gerber, P.; Hartman, P. G.; Hubschwerlen, C.; Locher, H.; Marty, H. P.; Stahl, M. *J. Med. Chem.* **2003**, *46*, 2304.
17. Otzen, T.; Wempe, E. G.; Kunz, B.; Bartels, R.; Yvetot, G. L.; Hänsel, W.; Schaper, K. J.; Seydel, J. K. *J. Med. Chem.* **2004**, *47*, 240.
18. Piper, J. R.; Johnson, C. A.; Maddry, J. A.; Malik, N. D.; McGuire, J. J.; Otter, G. M.; Sirotnak, F. M. *J. Med. Chem.* **1993**, *36*, 4161.
19. Gangjee, A.; Guo, X.; Queener, S. F.; Cody, V.; Galitsky, N.; Luft, J. R.; Pangborn, W. *J. Med. Chem.* **1998**, *41*, 1263.
20. Broughton, M. C.; Queener, S. F. *Antimicrob Agents Chemother.* **1991**, *35*, 1348.
21. Chio, L. C.; Queener, S. F. *Antimicrob Agents Chemother.* **1993**, *37*, 1914.
22. Glide, version 5.0, Schrödinger, LLC, New York, NY, 2008.
23. LigPrep, version 3.0, Schrödinger, LLC, New York, NY, 2008.
24. MarvinSketch version 5.2 ChemAxon Ltd, 2008.
25. Nu, H.; Kalyanaraman, C.; Irwin, J. J.; Jacobson, M. P. *J. Chem. Inf. Model.* **2006**, *46*, 243.
26. Jacobson, M. P.; Pincus, D. L.; Rapp, C. S.; Day, T. J.; Honig, B.; Shaw, D. E.; Friesner, R. A. *Proteins* **2004**, *55*, 351.
27. Yu, Z.; Jacobson, M. P.; Friesner, R. A. *J. Comput. Chem.* **2006**, *27*, 72.
28. Jaguar, version 8.0 Schrödinger, LLC, New York, NY, 2008.